Desalination and Water Treatment
www.deswater.com

doi:10.5004/dwt.2019.23670

145 (2019) 57–69
March

Performance evaluation of optimized carbon xerogel electrode in desalination through flow-electrode capacitive deionization: capacitance optimization by response surface methodology

Mahdi Alam[a,*], Seyed Amirodin Sadrnejad[a], Mohammad Reza Ghaani[b]

[a]*Department of Civil and Environmental Engineering, K.N. Toosi University of Technology, No. 1346, Vali Asr street, Mirdamad intersection, Tehran, Iran, Tel. +98(21)88779474, Fax +98(21)88779476, email: maalam@mail.kntu.ac.ir (M. Alam), sadrnejad@kntu.ac.ir (S.A. Sadrnejad)*
[b]*School of Chemical and Bioprocess Engineering, University College Dublin, Belfield, Dublin 4, Ireland, Tel. +353(1)7161812, email: mohammad.ghaani@ucd.ie (M.R. Ghaani)*

Received 12 February 2018; Accepted 20 December 2018

ABSTRACT

Capacitive deionization (CDI) is an energy efficient desalination method which is founded on the simple mechanism of ion attraction and repulsion by charged electrodes. One of the main challenges in implementation of this method in industrial scale is the synthesis of an optimum electrode material. Carbon gel is known to be one of the most promising candidates for the electrode material of CDI. Among different types of carbon gels, carbon xerogels have much lower costs of synthesis due to subcritical drying method used at the expense of reducing the porosity and specific capacitance. Here, we optimize carbon xerogel fabrication parameters using response surface methodology (RSM), in order to achieve maximum capacitance. Specifically, we focus our attention on investigation the effect of (i) the pH of initial RF solution, (ii) Reactant to liquid ratio of RF solution, and (iii) Pyrolysis temperature of dried carbon gel. Through our methodology, we show that with the choice of pH = 6.25, R/L = 30%, and PT = 736°C, an optimum capacitance of 42.26 F/g can be achieved. We then use this electrode in our FCDI cell and demonstrate that we can desalinate up to 87.7% a solution containing 1 g/L NaCl whit salt adsorption capacity of 7 mg/$g_{electrode}$.

Keywords: Water desalination; Capacitive deionization; Carbon xerogel; Response surface methodology

1. Introduction

Rapid population growth and an accelerating increase in water consumption per capita are two main factors affecting the higher-than-ever demand for clean water. Two-thirds of the global population (4.0 billion people) live under conditions of severe water scarcity at least 1 month of the year [1]. Water scarcity has already forced countries to consider unconventional waters to address the demand. The most important and widely used unconventional water is sea and brackish water desalination.

About 95% of operational water desalination plants are based on reverse osmosis (RO) or distillation methods such as multistage flash distillation (MFD) and multi effect distillation (MED) [2]. Both RO and distillation methods are energy intensive. In distillation methods, energy is needed for heating up water and also for needed electrical equipment such as pumps. In RO, which is much more energy efficient than distillation, most of the energy is consumed in high-pressure pumps. Recent technological advancement has significantly improved the efficiency of RO. Today, there are claims of energy cost of as low as 2.5 kWh for desalinating one cubic meter of saline water, which is about three times the theoretical minimum energy (aka thermodynamic energy) needed for the desalination of seawater [3]. But

*Corresponding author.

this, when combined with capital expenditure, is still high enough that only few rich countries afford RO-based desalination plants. This has motivated numerous new ideas and methods with the hope of decreasing the energy consumption and cost, and therefore affordability of desalination.

One of the most energy-efficient desalination methods is capacitive deionization (CDI), which has attracted a lot of attention in recent years particularly for desalination of brackish water.

In desalination through capacitive deionization, salt water passes through a pair of electrodes with positive and negative charges (the so-called CDI cell). Electrodes attract ions in water, which are in charge of salinity. With ions stuck next to electrodes, desalinated water flows out of the CDI cell.

The CDI was first introduced in early 1960s, and it was readily suggested that it might have important applications in desalination. But after just a few years, its development was halted due to the lack of understanding of the exact mechanism behind the CDI function [4]. It took years of research to demonstrate the double layer effects in porous electrodes and consequently the actual mechanism and model of ion removal in the CDI method were established.

About three decades later (late 1990s), after the work of Farmer and co-workers on "Capacitive Deionization with Carbon Aerogel Electrodes" [5] an increasing number of studies and publications focused on CDI and specially the CDI electrode materials. Since then, carbon aerogels as an active electrode material, have always been in the forefront of attention and research in super capacitors and CDI system due to their (i) monolithic network structure, (ii) high conductivity, and (iii) high accessible surface area.

In the synthesis of carbon aerogels, drying method of the initial gel is the most important stage and typically time and cost intensive. Carbon gels synthesized from different drying methods are called with different names such as carbon aerogel, carbon xerogel and carbon cryogel. Among these different types of carbon gels, carbon xerogel (obtained through subcritical drying) is more cost-efficient since its synthesis is simpler and does not require specialized equipment. Nevertheless, this saving comes at the expense of reduction in porosity and specific capacitance.

Here, we investigate details of carbon xerogel synthesis and optimize the parameters involved in the synthesis procedure in order to obtain a cost-effective electrode material for using in capacitive deionization. The goal is to develop a more efficient electrode which is also commercially competitive with commonly used activated carbon. For the optimization of the porosity and the capacitance of our synthesized electrodes, we use Box-Behnken method for the design of our experiments along with response surface methodology for optimization. The three involved parameters are (i) the pH of initial resorcinol-formaldehyde (RF) solution, (ii) Reactant to liquid ratio (R/L) of RF solution, and (iii) Pyrolysis temperature (PT) of dried carbon gel. We finally, use our fabricated optimum electrode in a flow electrode capacitive deionization cell for desalination of brackish water and demonstrate that it is more efficient than available commercial activated carbon electrodes.

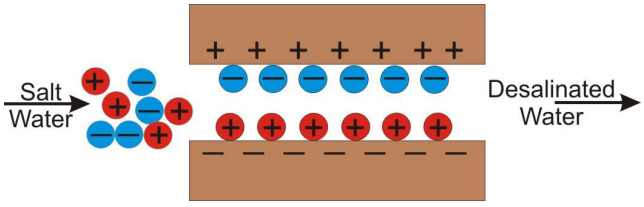

Fig. 1. Schematic of mechanism of capacitive deionization (CDI). Positive and negative ions of salt water, as it enters a CDI cell, are attracted to respectively negative and positive electrodes. Water with no ions, i.e. desalinated, exits the other end of the cell.

2. Materials and methods

2.1. Synthesis of carbon xerogel

Synthesis of carbon xerogel is composed of four main steps: 1 - Preparing the initial RF solution, 2 - Gelation, 3 - Drying and 4 - Pyrolysis.

1 - Preparing the initial RF solution: Needed initial solution is composed of resorcinol (99%, Merck KGaA, Germany) and formaldehyde (37%, Merck KGaA, Germany) with 2:1 molar ratio. We then add the catalyst, sodium carbonate (99%, Merck KGaA, Germany), whose volume will be varied in this research. The amount of the catalysis is typically reported as the molar ratio of resorcinol to the catalyst (R/C), whose value for sodium carbonate has been chosen from R/C = 50 to 3000 [6–14], but can fall outside this range. The catalyst is not necessary, but extremely speeds up the time required for bond-formation between the two involved reactants (i.e. resorcinol and formaldehyde). Hence with the addition of the catalyst, the gelation time decreases considerably.

2 - Gelation: To obtain the desired carbon gel, the initial solution must be treated thermally. There is a wide range of possibility for such treatment, e.g. Gelation temperature ranges between 80 to 90°C, and 2–5-d duration [8,9,15–19] here following Saliger et al. [20], we choose to keep the solution at 25°C for one day, then at 50°C for another full day, and eventually at 90°C for 3 d.

3 - Drying: The obtained gel, contains a large volume of water within the network of bonded resorcinol and formaldehyde. To obtain the final porous carbon gel, we need to get rid of the water in the structure. This is done through the process of drying. There are three main methods for drying: (i) drying in subcritical condition (slow drying in ambient pressure) that yields the so-called xerogel, (ii) Supercritical drying that results in aerogel, and (iii) Freeze drying that gives cryogel, xerogel, aerogel and cryogel have similar raw ingredients, but their properties such as porosity, conductivity and capacitance are different. For example aerogel and cryogel have a higher porosity (i.e. more suitable for super-capacitors and CDI), but clearly are a lot more expensive to produce.

Here, for drying our carbon xerogel samples in ambient pressure, to avoid large shrinkage due to surface tension of water during evaporation, we try to exchange the water with other solvent like acetone. For this purpose, the wet gels are immersed in acetone for 24 h and during this time the acetone is changed twice. After that, the samples are dried in ambient temperature for 48 h.

4 - Pyrolysis: Dried gel, then, is heated in a tube furnace under the flow of a noble gas such as Nitrogen or Argon (or otherwise the dried gel will be oxidized). The purpose is for the dried gel to undergo "Pyrolysis" through which large organic molecules are decomposed into smaller ones. Prior literature have reported very wide range of temperature (600–1200°C) and duration time (1–5 h) [12–14,20–26]. Here, we have chosen 3-h duration (like most of mentioned researches), and temperature is varied for the purpose of optimization from 600 to 900°C.

In practice, room-temperature argon is injected into our furnace with the flow rate of 20 cm^3/min. We first gradually heat up the furnace (while argon is flowing) from the room temperature to intended temperature through these steps: 25 (room temperature)-300°C in 30 min, 300–600°C in 45 min, and for higher temperatures with the rate of 5°C/min (e.g. 600–900 in 60 min). Then, we keep the furnace at intended temperature for three additional hour for the pyrolysis to complete.

2.2. Parameters affecting the properties of carbon xerogels

According to the synthesis procedure described above, main parameters affecting the quality of the final carbon xerogel sample are (i) Resorcinol/formaldehyde molar ratio, (ii) Catalyst type, (iii) Resorcinol/catalyst molar ratio, (iv) pH, (v) Reactants/liquid mass ratio, (vi) Gelation temperature, (vii) Gelation time, (viii) Pyrolysis temperature and (ix) Pyrolysis time. Among these parameters, the pH of initial solution (that has a direct relationship with the amount of catalyst), the reactants/liquid mass ratio (R/L) and pyrolysis temperature (PT) are the most important parameters that were mentioned in various literatures [7,8,12,14,27–29], and therefore we choose these as the parameters of interest in this study. We choose the range of these three parameters according to Table 1 which is consistent with the prior experimental studies on this subject.

Initial pH of resorcinol-formaldehyde (37%) solution is 3.87 which will be increased by adding the catalyst. Due to the small volume of our samples (20 cc), adding slight amount of catalyst results in large changes in the pH. Therefore, to achieve the exact desired pH for every single tests, we use the standard curves of pH. For this purpose, we prepared different resorcinol-formaldehyde-catalyst (RFC) samples using 0.05 molar solution of Na_2CO_3 and for each R/L ratios we plot the obtained pH against the volume of catalyst solution (see Fig. 2). Using these standard curves we find the exact amount of catalyst solution needed for achieving the desired pH of our RFC samples (5.5, 6.25 and 7.0).

Table 1
Experimental variables and their coded levels for Box-Behnken design

Experimental variables	Symbol	Coded levels		
		–1	0	1
Initial pH of RFC solution*	pH	5.50	6.25	7.00
Reactant to liquid weight ratio (%)	R/L	30	40	50
Pyrolysis temperature (°C)	PT	600	750	900

* RFC solution: resorcinol-formaldehyde-catalyst solution

2.3. Research method (Experimental design and data analysis)

Traditionally, in order to study the effect of N number of parameters on the target function, researchers used to vary one-factor-at-a-time. In this method, one parameter is varied while others are kept constant and the optimum value of this variable is determined. This optimum value is then used to find other optimum parameters one by one. If M different values of each parameter is investigated, then the total optimization, requires N×M experiments. Clearly, the method of one-factor-at-a-time does not consider interactive effects entirely, and therefore does not necessarily converge to the global optimum of the phase space. Full factorial design of experiments is the most accurate method for considering all variables interactions, in which a matrix of all possibilities and therefore M^N experiments requires to be conducted.

A more modern approach is using some fractional factorial design of experiments and applying a multivariate statistical techniques to explore the relationship between the variables and the response or responses. For this purpose, the so-called response surface methodology (RSM) is one of the most popular techniques among scientists. The method of RSM, through a series of mathematical and statistical techniques, expresses the objective function as an algebraic polynomial equation of all involved parameters of the system [30]. Specifically, the output of RSM is a quadratic polynomial in the form

$$Y = \beta_0 + \sum_{i=1}^{k}\beta_i X_i + \sum_{i=1}^{k}\beta_{ii}X_i^2 + \sum_{i=1}^{k-1}\sum_{j=i+1}^{k}\beta_{ij}X_iX_j + \varepsilon \quad (1)$$

in which k is the number of parameters, β_0 is the intercept constant or constant term of equation and β_i, β_{ii} and β_{ij} are respectively coefficients of linear, quadratic and interaction parameters. X denotes the independent variables, Y is the response parameter and is residual associated to the experiments.

To arrive at the above expression, first a specific number of experiments must be conducted. There are different meth-

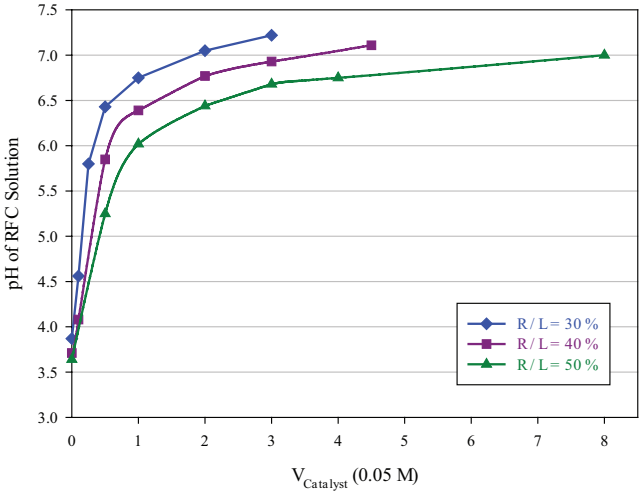

Fig. 2. Standard curves for achieving desired pH for different reactant to liquid ratios (R/L).

odologies that suggest how this initial set of experiments must be selected, i.e. what parameters must be varied and how to vary them. Here, considering our continuous-type parameters and the specific range of them, we choose to use Box-Behnken method to design our experiments. This set of experiment is listed in Table 2.

After conducting the aforementioned 15 experiments, in order to investigate the fitting quality (or the quality of fitted model) we use the table of ANOVA (analysis of variance) together with R^2 and adjusted R^2. The lower the P-value in the ANOVA table, the higher the fitting quality. Higher values of R^2 and adjusted R^2 further confirm the quality of fitting. Another quality control test for our model is the "lack of fit" test that as its name suggests is a measure of the difference between experimental data and the model estimations. Lack of fit is usually more significant when we have to drop interaction or quadratic terms in our model due to their P-value being large, or if there are very large residuals. If our model represents a good fit, P-value of the lack-of-fit must be greater than 0.05 which means the lack-of-fit is insignificant. Finally, for verification of our model within the specified range of variables we perform three additional experiments. We present the effect of involved independent variables and their interactions on the response parameter via three-dimensional response surfaces. These surfaces enable us to deduce values of variables that correspond to the optimum response parameter.

2.4. Measuring the specific capacitance of electrodes

For performance evaluation of electrodes in the method of CDI, typically two different approaches are pursued: 1- The salt water is passed over a pair of electrodes and the decrease in salinity is measured, 2- Electrode specifications is determined through measurement of voltage and amperage in a three-electrode configuration composed of a reference electrode, a counter electrode and working electrode. The three electrodes are placed into the electrolyte, an electrical potential-difference is applied between the references and working electrode, and the current is measured by the counter electrode. In this approach, capacitance of electrodes can be calculated through cyclic volt ammetry (CV) or electrochemical impedance spectroscopy (EIS). Here we use the former methodology (CV), in which capacitance is calculated from the electrode charge. Electrode charge in a specific voltage range is given by

$$Q = \int I\,dt = \int \left[I(v)dv \times \frac{dt}{dv} \right] = \frac{\int I(v)dv}{\frac{dv}{dt}} = \frac{\int I(v)dv}{r}. \quad (2)$$

The term $r = \frac{dv}{dt}$ is called scan rate which is the rate of change of voltage in time. Capacitance (C) is related to charge and voltage through $= \frac{Q}{V}$, and since in cyclic volt ammetry (CV) the current is plotted in charging and discharging modes, capacitance of electrodes in electrolyte can be calculated by

$$C = \frac{\int I(v)dv}{2r\Delta V}, \quad (3)$$

in which $\int I(V)dv$ is the area under CV curve in the considered voltage range (ΔV).

Since our samples weigh differently and in order to be able to compare their capacitance, we normalize the above relation [Eq. (3)] with the mass of the working electrode which obtains capacitance per unit mass, i.e.,

Table 2
The Box-Behnken design matrix for experimental variables and the response values

Standard order	Run order	Variables						Responses	
		X_1 pH		X_2 R/L (%)		X_3 PT (°C)		Y_1 Density	Y_2 Capacitance
		Coded	Actual value	Coded	Actual value	Coded	Actual Value	g/cm^3	F/g
14	1	0	6.25	0	40	0	750	0.466	26.57
5	2	–1	5.50	0	40	–1	600	0.557	0.99
2	3	1	7.00	–1	30	0	750	1.023	7.44
3	4	–1	5.50	1	50	0	750	0.746	5.78
6	5	1	7.00	0	40	–1	600	1.213	0.36
9	6	0	6.25	–1	30	–1	600	0.396	17.28
13	7	0	6.25	0	40	0	750	0.480	26.22
8	8	1	7.00	0	40	1	900	1.441	1.99
15	9	0	6.25	0	40	0	750	0.464	29.35
10	10	0	6.25	1	50	–1	600	0.732	0.76
12	11	0	6.25	1	50	1	900	0.767	27.65
7	12	–1	5.50	0	40	1	900	0.527	4.38
4	13	1	7.00	1	50	0	750	1.243	0.92
1	14	–1	5.50	–1	30	0	750	0.270	6.49
11	15	0	6.25	–1	30	1	900	0.439	11.04

$$C = \frac{\int I(v)dv}{2m\ r\Delta V}. \quad (4)$$

Here, in our experiments for performing CV tests, we use a potentiostat (μAutolabIII, Metrohm, the Netherlands) with a platinum wire for the counter electrode, and Ag/AgCl for the reference electrode, and all experiments are conducted at 10 mV/s scan rate. Our electrolyte is an aqueous solution of NaCl (0.5 M), which is chosen here - as is common in similar research [31–34] to resemble saline water in the nature.

2.5. Construction of the laboratory scale FCDI unit

The FCDI cell, which is used in our research to determine the desalination capacity of xerogels, is composed of two 20×15 rectangular-shape current collectors made up of stainless steel (grade 316). In order to let the flow electrode to pass and hence get charged, on the surface of each of these current collectors we carve a flow channel of depth 2.5 mm and the total length 175 cm. Next to these two current collectors, there are cation and anion exchange membranes (Fig. 3). In the middle of our unit, there is a silicone gasket of thickness 3 mm in which we cut an opening of 10×15 cm by laser cutter. We place a polyester spacer in the area inside the silicone gasket (where brackish water flows). Three peristaltic pumps inject flow electrodes and brackish water to FCDI unit with respective volume flow rates of 25 and 15 cc/min from respectively 250 cc and 100 cc reservoirs. Our FCDI cell works in a batch mode, and flow electrodes and desalinated water are returned to the reservoirs after deionization. We apply a 1.2 V electric potential to our current collector and monitor the salinity continuously through anECmeter (HTA, AZ-8603). In order to use our optimum xerogel as flow electrode in FCDI, these electrodes are ground by ball mill to an average diameter of 200 microns.

2.6. Performance evaluation of synthesized carbon xerogel

Several categories of carbon materials are used as electrode material for application in CDI. These include, for instance, activated carbon (AC), carbon aerogels (CA), carbon nano tubes (CNT), carbon nano fibers (CNF) and graphene. There is an on-going research to increase the capacitance of these electrodes, hence their efficiency, through alternative synthesizing process or by making the composites with different kind of carbon materials and metal oxides. Nevertheless, as of today the most common electrode material is yet the activated carbon, which is easy to synthesize, and therefore is cheap and available off the shelf.

As mentioned earlier, the goal here is to achieve a new electrode material that has a higher efficiency than that of activated carbon, but is also easy to synthesize. If achieved, this new material offers a better alternative to activated carbon.

To find the optimum carbon xerogel, as elaborated in section 2.3. and 2.4., we synthesized a variety of carbon xerogel samples under different synthesis conditions, and compared their capacitance obtained via cyclic voltammetry. The optimum xerogel obtained through this process must be compared with activated carbon in order to quantitatively assess its potential advantage. Nevertheless, activated carbon is only available in a powder or granular form and thus we cannot use cyclic voltammetry to directly measure its capacitance. Therefore, we grind the optimum synthesized carbon xerogel and compare its efficiency in desalination with activated carbon in our FCDI laboratory pilot. To do so, we target desalination of a solution with salinity of 1 g/L, and plot the normalized total dissolved solid as a function of time for (i) electrode made of our optimum carbon xerogel and (ii) the activated carbon sample. To make sure that the results are repeatable (test-retest reliability), we repeat each test for three times.

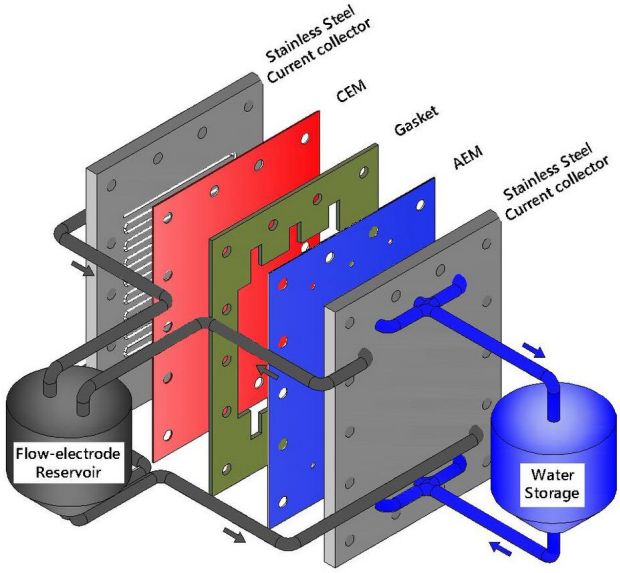

Fig. 3. The schematic of our laboratory scale FCDI unit.

3. Results and discussion

To post process our experiments, we first determine the density of our samples (see Table 1) by measuring their weights, diameters and thicknesses. Since a lower density corresponds to a higher porosity that potentially can result in higher capacitance, our objective is to minimize the density. As discussed above, here we use the method of RSM to find parameters that achieve this objective. Coefficients of our model's second-order polynomials are then found through statistical analysis of our experimental results. These coefficients in coded and actual value forms are

$$Y = 0.4701 + 0.3525X_1 + 0.1701X_2 + 0.0346X_3 + 0.3506X_1^2 + 0.1137X_3^2 - 0.0640X_1X_2 + 0.0647X_1X_3 \quad (5)$$

$$Density = 24.43 - 7.411pH + 0.0703R/L - 0.01094PT + 0.6233pH^2 + 0.000005PT^2 - 0.00853pH \times R/L + 0.000575pH \times PT \quad (6)$$

Clearly, a positive coefficient in Eq. (5) indicates that the parameter increases the response parameter (which here is the density) and hence is working against the optimization.

Likewise, a negative coefficient helps decreasing the density. Also, magnitude of the coefficient of each parameter in the coded equation is a measure of how important the effect of that parameter is on the response parameter.

As result of ANOVA in Table 3 shows, our model's P-value is very small (<0.001) which indicates that our constructed model is significant. Also, values of parameters R^2 and adjusted R^2 are very close to unity which is another positive indicator of fitting quality. However, P-value of the lack-of-fit parameter is less than 5% which is mainly due to few results having large residuals. To investigate this matter further, we performed three experiments for various values of parameters within our specified range (see Table 5), and observed errors of 5.9% to 13.53% which are relatively large errors. To address this issue, we chose to invoke the method of data transformation. Here, we reconsider our model by choosing Lambda = 0. With this strategy, not only P-value of our model stayed at the same small value of 0.001, but also P-value of the lack-of-fit parameter increased to 0.723 which is an indicator of insignificance of the lack-of-fit. Also parameters R^2 and adjusted R^2 exceeded the very good threshold of 99.9% (Table 4). Furthermore, our verification experiments show a response with a much less error compared to the cases without data transformation (see Table 5).

The new second-order polynomial equation in coded and actual value forms read

$$\begin{aligned} Ln(Y) = {} & -0.7548 + 0.4533X_1 + 0.2981X_2 + 0.0334X_3 \\ & +0.4144X_1^2 + 0.1733X_3^2 - 0.2055X_1X_2 + 0.0570X_1X_3 \\ & -0.0140X_2X_3 \end{aligned} \quad (7)$$

Table 3
Analysis of variance (ANOVA) of RSM quadratic model terms for density

Source	DF*	Adj SS**	Adj MS***	F-Value	P-Value
Model	7	1.75381	0.250545	117.43	<0.001
Linear	3	1.23488	0.411627	192.93	<0.001
pH	1	0.99383	0.993835	465.82	<0.001
R/L	1	0.23146	0.231471	108.49	<0.001
PT	1	0.00957	0.009574	4.49	0.072
Square	2	0.48585	0.242923	113.86	<0.001
pH×pH	1	0.45653	0.456531	213.98	<0.001
PT×PT	1	0.04798	0.047979	22.49	0.002
2-Way Interaction	2	0.03309	0.016544	7.75	0.017
pH×R/L	1	0.01636	0.016362	7.67	0.028
pH×PT	1	0.01673	0.016725	7.84	0.027
Error	7	0.01493	0.002134		
Lack-of-Fit	5	0.01478	0.002957	38.90	0.025
Pure Error	2	0.00015	0.000076		
Total	14	1.76875			
R^2	0.9916				
Adjusted R^2	0.9831				

*Degree of freedom
** Some of squares
*** Mean of squares

$$\begin{aligned} Ln(Density) = {} & 22.461 - 7.888pH + 0.20803R/L \\ & -0.014122PT + 0.7367pH^2 + 0.000008PT^2 \\ & -0.02739pH \times R/L + 0.000507pH \times PT \\ & -0.000009R/L \times PT \end{aligned} \quad (8)$$

Further quality assessment of our model is provided in supplementary document (Section I).

Now that we have confidence in our model, we move on to investigate the effect of each parameter on the response. Since there are three parameters affecting the response, a four-dimensional surface is needed to visualize the functionality. Since this is not possible, we investigate the effect of each pair of two parameters in one of the three-dimensional plots of Fig. 4. Lower PH and R/L results in a carbon xerogel of lower density, and the lowest density attainable is for a pyrolysis temperature somewhere between the max/min of our temperature range. We would like to note that our experiments suggest that the effect of pyrolysis temperature on the density is in fact very small which is also confirmed by optimization plots of Fig. 5. Based on these optimization plots, minimum of density (or equivalently maximum porosity) is achieved at pH = 5.65, R/L = 30% and PT = 748°C. These values are very close to one of our experiments and therefore we can conclude that the density of 0.27 g/cm^3 is the minimum achievable density within the chosen range. Since the skeleton density of carbon xerogel is 1.5 g/cm^3 [27,35], therefore, the porosity of our optimum sample (that has the minimum density) is 82%.

We note here that our original motivation for minimizing the density (or maximizing porosity) was to

Table 4
Analysis of variance (ANOVA) of RSM quadratic model terms for density with transformation (Lambda = 0)

Source	DF*	Adj SS**	Adj MS***	F-Value	P-Value
Model	8	3.26160	0.40770	1702.17	<0.001
Linear	3	2.36416	0.78805	3290.16	<0.001
pH	1	1.64416	1.64416	6864.48	<0.001
R/L	1	0.71107	0.71107	2968.75	<0.001
PT	1	0.00892	0.00892	37.25	0.001
Square	2	0.71482	0.35741	1492.20	<0.001
pH×pH	1	0.63775	0.63775	2662.62	<0.001
PT×PT	1	0.11152	0.11152	465.62	<0.001
2-Way Interaction	3	0.18263	0.06088	254.16	<0.001
pH×R/L	1	0.16885	0.16885	704.97	<0.001
pH×PT	1	0.01299	0.01299	54.23	<0.001
R/L×PT	1	0.00078	0.00078	3.28	0.12
Error	6	0.00144	0.00024		
Lack-of-Fit	4	0.00076	0.00019	0.56	0.723
Pure Error	2	0.00068	0.00034		
Total	14	3.26304			
R^2	0.9996				
Adjusted R^2	0.9990				

* Degree of freedom
** Some of squares
*** Mean of squares

Table 5
Verification tests for density

Variables						Response (density)				
X_1 pH		X_2 R/L (%)		X_3 PT (°C)		Experimental	Model	Error	Model	Error
Coded	Actual Value	Coded	Actual Value	Coded	Actual Value	g/cm^3	No transformation	Percentage	Lambda = 0	Percentage
–1	5.50	–0.5	35	–1	600	0.436	0.495	–13.53	0.425	2.52
–1	5.50	1	50	0	750	0.746	0.702	5.90	0.748	–0.29
0	6.25	–0.5	35	0	750	0.416	0.385	7.44	0.405	2.64

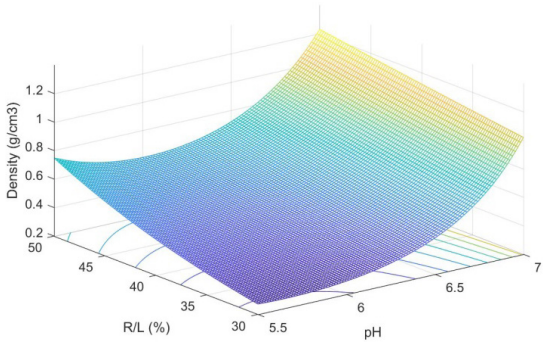

(a)

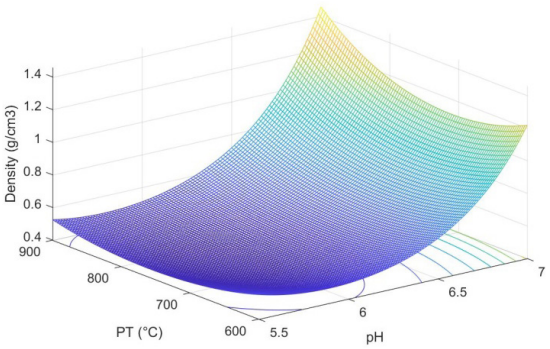

(b)

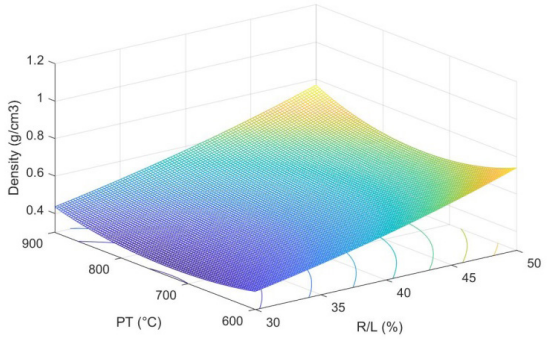

(c)

Fig. 4. Three-dimensional surface plots of our synthesized carbon xerogels for density as a function of a) pH and R/L (hold value: PT = 750°C), b) pH and PT (hold value: R/L = 40%), c) R/L and PT (hold value: pH = 6.25).

maximize capacitance such that our carbon xerogel has a higher efficiency in CDI desalination method. In order to see whether density and capacitance, as we assumed, are related, we plot the CV curve of all samples by potentiostat. We show, in Fig. 6, CV curves of one of our samples for different scan rates. For all scan rates the curves are nearly symmetric and therefore we can conclude that the charging and discharging are reversible. This symmetric behavior also suggests that the electrodes behave the same when used as anode or cathode, at least in the considered range of voltage. Furthermore, we observe no gas bubbles near the samples during the measurement and no redox or faradic reaction peaks in CV curves. It is to be noted that the mere absence of gas bubble near electrodes during the test – while is a necessary condition for no Faradaic reaction – but it is not sufficient and more specific tests are needed to elucidates further details about possibility and volume of Faradaic reactions.

Finally, we calculate capacitance of all samples from CV curves obtained at the scan rate of 10 mV/s (Table 2). Here, similar to the case of densities, the best fitted model is obtained from data transformation with lambda = 0. The second order polynomial for this model in the coded and actual-value form are, respectively,

$$\begin{aligned} Ln(Y) &= 3.3086 - 0.4389X_1 - 0.5515X_2 + 0.7938X_3 \\ &\quad -1.8571X_1^2 - 0.0645X_2^2 - 1.1700X_3^2 - 0.4938X_1X_2 \\ &\quad +0.0590X_1X_3 + 1.0104X_2X_3 \end{aligned} \tag{9}$$

$$\begin{aligned} Ln(Capacitance) &= -147.84 + 42.924pH - 0.0973R/L + 0.05307PT \\ &\quad -3.3016pH^2 - 0.000645(R/L)^2 - 0.000052PT^2 \\ &\quad -0.06583pH \times R/L + 0.000524pH \times PT \\ &\quad +0.000674R/L \times PT \end{aligned} \tag{10}$$

As shown in the results of variance analysis (ANOVA, see Table 6), our model has a P-value < 0.001 that implies that our model is significant. The lack-of-fit parameter, considering the large P-value, is insignificant, and close-to-unity values of R^2 and adjusted R^2 is another confirmation that our model is a good fit.

For verification of our model, similar to what we did for densities, we conduct three more experiments whose results are listed in Table 7. Results of verification experiments match very well with the model predictions, and this serves as another check for the adequacy and validity of our model. Further quality assessment of this model is provided in supplementary document (Section I).

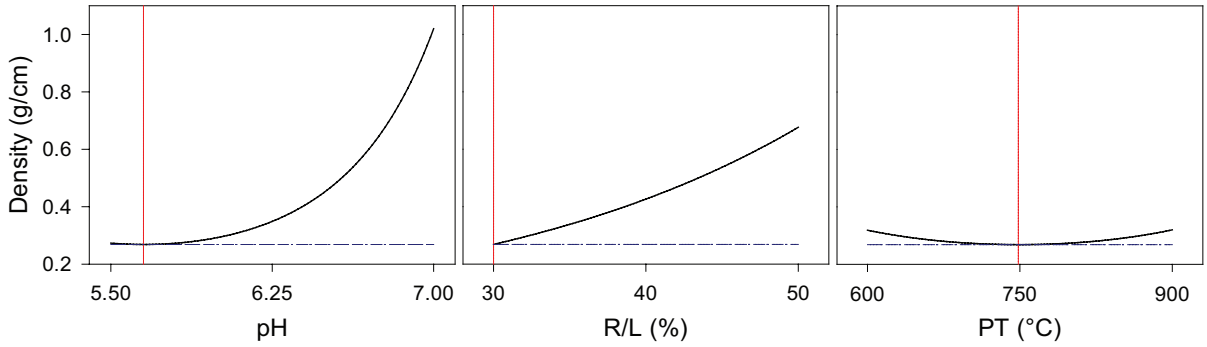

Fig. 5. Optimization plots for minimizing the density of our synthesized carbon xerogels. Optimum conditions: pH = 5.65, R/L = 30%, PT = 748.5°C and minimum achievable density = 0.2685 g/cm^3.

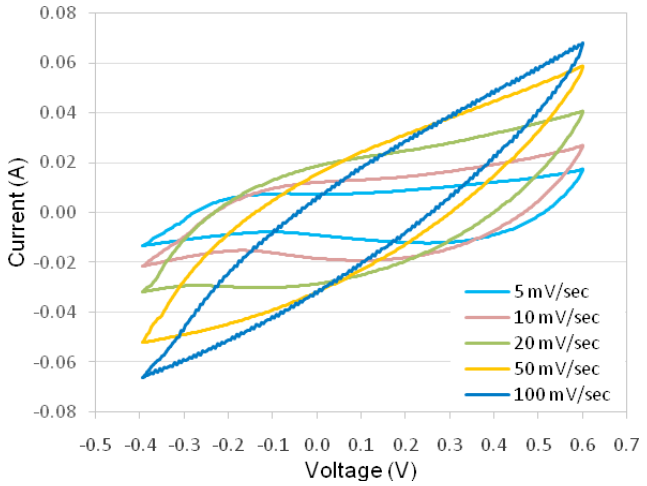

Fig. 6. Cyclic voltammetry diagram for one of synthesized carbon xerogels at different scan rates.

Table 6
Analysis of variance (ANOVA) of RSM quadratic model terms for capacitance with transformation (Lambda = 0)

Source	DF*	Adj SS**	Adj MS***	F-Value	P-Value
Model	9	30.8280	3.4253	1793.62	<0.001
Linear	3	9.0154	3.0051	1573.59	<0.001
pH	1	1.5413	1.5413	807.10	<0.001
R/L	1	2.4328	2.4328	1273.90	<0.001
PT	1	5.0413	5.0413	2639.78	<0.001
Square	3	16.7395	5.5798	2921.78	<0.001
pH×pH	1	12.7345	12.7345	6668.20	<0.001
R/L× R/L	1	0.0154	0.0154	8.04	0.036
PT×PT	1	5.0548	5.0548	2646.87	<0.001
2-Way Interaction	3	5.0731	1.6910	885.48	<0.001
pH×R/L	1	0.9752	0.9752	510.63	<0.001
pH×PT	1	0.0139	0.0139	7.29	0.043
R/L×PT	1	4.0840	4.0840	2138.53	<0.001
Error	5	0.0095	0.0019		
Lack-of-Fit	3	0.0019	0.0006	0.17	0.908
Pure Error	2	0.0076	0.0038		
Total	14	30.8375			
R^2	0.9997				
Adjusted R^2	0.9991				

*Degree of freedom
** Some of squares
*** Mean of squares

For visualizing the interactive effects of factors on the response (electrode capacitance), in Fig. 7, we fix one of the three parameters and plot the response as a function of the other two parameters. Generally, as R/L decreases (across the range of PH) capacitance increases, and a pH~6.25 (which is nearly in the middle of our range for pH) gives the maximum capacitance (see Fig. 7a). From Fig. 7b it is seen that the optimum PT is about 750°C and at the same pH~6.25. Optimum values obtained from Fig. 7c are consistent with the above values. The optimum response can also be obtained from our polynomial model, which gives pH~6.25, R/L = 30% and PT = 736°C (Fig. 8).

With the obtained optimum values for parameters in hand, we proceed to synthesize the sample. Our final sample has a capacitance of 42.26 F/g, which is very close to the prediction of our model which is 44.96.

We would like to note here that while Fig. 8 suggests that lower values of R/L result in higher capacitance, it is practically not possible to go very much below the threshold value of R/L = 27%–28%. This is because for R/L values below this threshold, gelation does not occur anymore. For instance, for R/L = 20% and for low pH (that is lower amount of catalyst) after curing stage, the resolsinol-formaldehide polymer does not form, and therefore the final gel will not be obtained. In this case, in order to get the polymer, we must add more catalyst or increase the curing time. Increasing the catalyst will result in significant decrease in porosity and capacitance. Increase in the curing time increases the cost and required time. Either of these two solutions pushes us away from our objective, which is a cost-effective and fast fabrication process for high-capacitance electrodes.

After synthesizing of the final optimum electrode with the maximum capacitance, we would like to investigate its performance in CDI and to compare it with activated carbon. To do so, we grind our synthesized electrode by a ball mill to 200 micron in diameter and use this electrode powder in our FCDI cell to investigate its performance in an actual desali-

Table 7
Verification tests for capacitance

Variables						Response (capacitance)		
X_1 pH		X_2 R/L (%)		X_3 PT (°C)		Experimental	Model Lambda = 0	Error
Coded	Actual value	Coded	Actual value	Coded	Actual value	F/g	F/g	Percentage
–1	5.50	–0.5	35	–1	600	1.62	1.65	–1.85
–1	5.50	1	50	0	750	5.86	5.86	–1.38
0	6.25	–0.5	35	0	750	35.45	35.45	–3.29

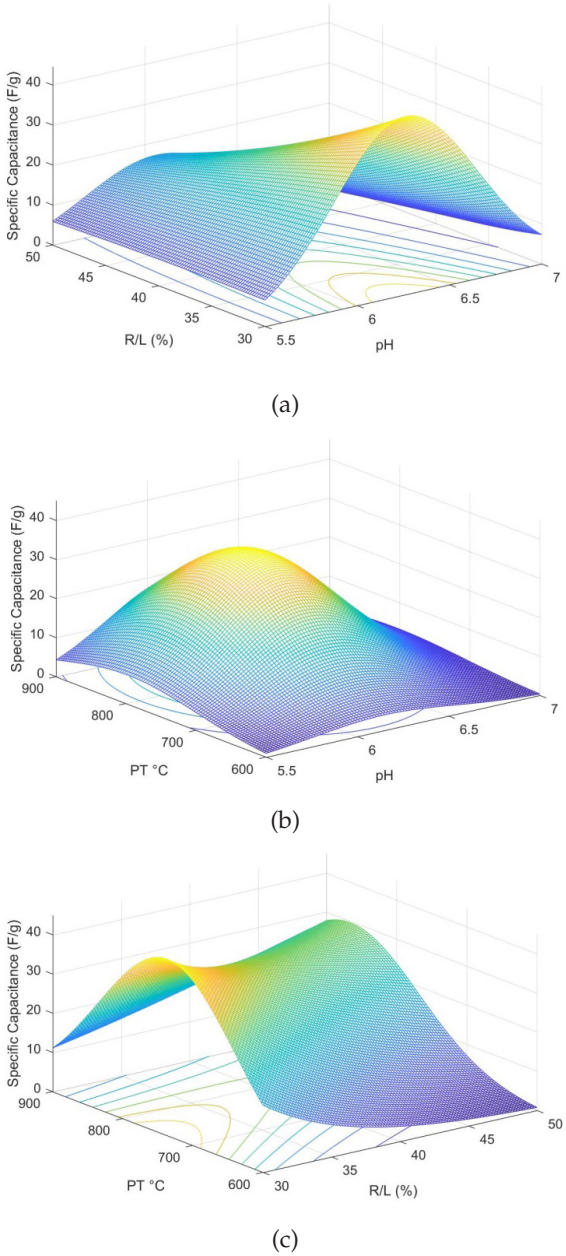

(a)

(b)

(c)

Fig. 7. Three-dimensional surface plots of our synthesized carbon xerogels for capacitance as a function of a) pH and R/L (hold value: PT = 750°C), b) pH and PT (hold value: R/L = 40%), c) R/L and PT (hold value: pH = 6.25).

nation. We prepare a 5 wt% of powdered carbon xerogel and activated carbon (Norit D 10) suspension in a 0.1 M NaCl solution. In order to avoid the settlement of our powder electrode and hence stability of our suspension, we add a 0.2 wt% dispersant. To check the performance of this strategy, we ran one of our tests for more than 30 h and closely monitored the outflow of the electrode suspension. No noticeable change was observed during this entire period, and the flow-rate stayed at the same 25 ml/min. This is an indication that there is no major settlement of electrode suspension in flow channels of our FCDI pilot. Note that if there is particle settlement in channels, the effective diameter of the channel is reduced and therefore the flow must be reduced. As a further check, after we dismantled our apparatus at the end of the experiments, we examined the channels for any potential clogging caused by settlement, but nothing was found.

Water with salinity of 1 g/L is continuously pumped between the two steel current collectors of our FCDI cell (which is designed in the batch mode). Water, after each round of desalination, re-enters the reservoir and therefore the salinity of reservoir decreases over time as shown in Fig. 9. As can be seen from this figure, decreasing rate of salinity, as expected, reduces over time. In our experiment, after 6.5 h more than 87% of the salt has been removed from the water. Salt adsorption capacity (SAC) here is about 7 $mg/g_{electrode}$ which shows about 9% higher performance than commercially available activated carbon.

Finally, we would like to comment about the performance of the FCDI method for desalination of higher salinity solutions. To quantitatively address this, we consider a solution with salinity of 5 g/L, and put it under desalination with our FCDI pilot for 6 h. Salinity of this solution decreases to about 42% of its initial salinity in this 6-h period (Fig. 10). For performance comparison of the FCDI pilot for different salinity, we also plot in Fig. 10 the salinity reduction as a function of time for a 1 g/L solution, which reduces to about 13% of its initial salinity over the 6-h period. Note that for both solutions, the experiment has stopped at t = 6 h. But non-zero slope of both curves at t = 6 h shows that allowing more time can result in lower salinity of the final solution. Therefore, FCDI can desalinate saltier solutions, although for a similar normalized reduction (salt reduction percentage) we will need more time. It is to be noted that higher effective surface between the solution and electrode suspension clearly increases the performance of desalination, and salt reduction can be achieved in a proportionally shorter time.

We were also interested to investigate whether any chemical reaction occurs during our desalination. This is

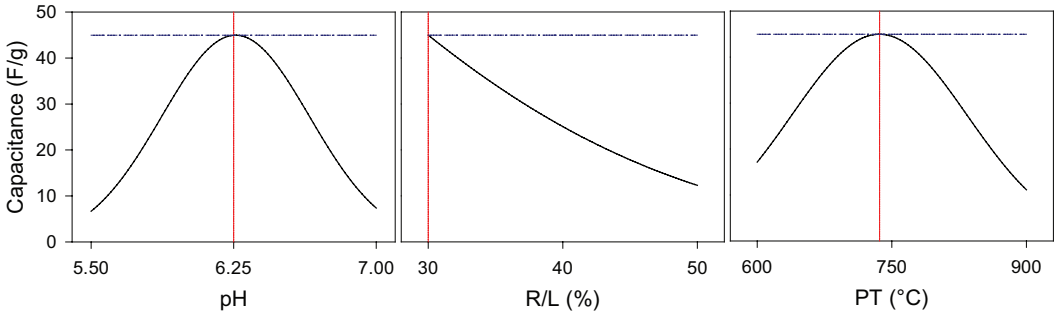

Fig. 8. Optimization plots for maximizing the capacitance of our synthesized carbon xerogels. Optimum conditions: pH = 6.25, R/L = 30%, PT = 736°C and maximum achievable capacitance = 44.96 F/g.

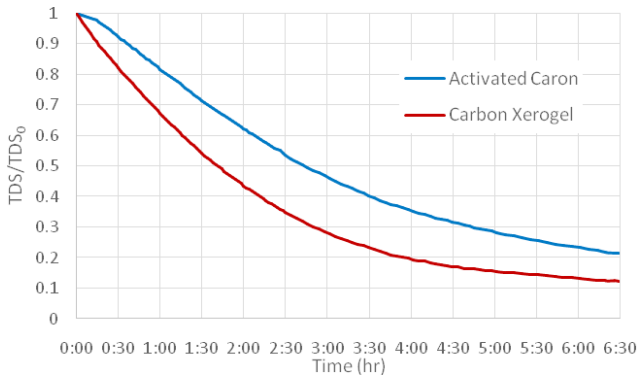

Fig. 9. Desalination performance of our optimum carbon xerogel compared with commercially activated carbon in a batch mode flow-electrode capacitive deionization system.

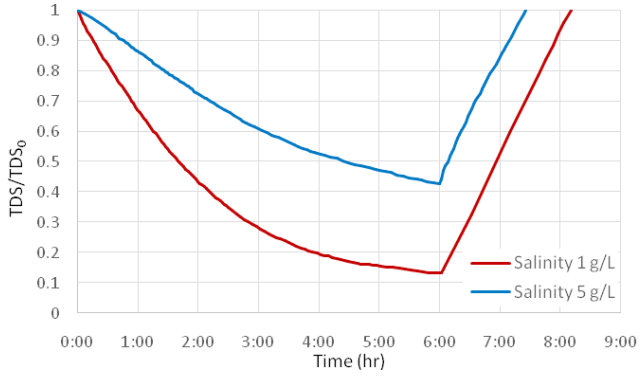

Fig. 10. Desalination and salination comparison of different water salinity (1 and 5 g/L) in our FCDI apparatus.

important for the regenerability of the electrodes. To answer this question, we reversed the current in both experiments (i.e. for 5 g/L and 1 g/L solutions) at t = 6 h to observe the process of ions repulsion from electrodes (Fig. 10). Our experiments show that the time needed for ions to return to the solution is about one third of the time needed for their removal from the solution, i.e. salination time is 1/3 of desalination time. Please note that the slopes of the curves at the end of "salination" (i.e. at t ≈ 7.5, 8.15 h respectively for 5 and 1 g/L solutions) are finite (non-zero) values, which is due to initial salinity of our electrodes (0.1 M NaCl ≈ 5.8 g/L). Therefore, if we do not stop the process, the final salinity of our solution can exceed its initial salinity.

At the end of the experiment, we measured the salinity of both the solution and our electrode suspension. The final salinity of both was the same as the initial salinity. We conducted this cycle for three times and the results were the same in all of them. We also measured the pH of solution in a few steps during our tests and no noticeable changes were observed. Although these are positive signs of the electrostatic adsorption of ions by our electrodes during desalination or regeneration process, but to make a definite statement about the occurrence of oxidation or Faradaic reactions on electrodes, these three tests are not sufficient and the tests should be carried out for much more time. Variation of electrical conductivity of solution as a function of time for the cycles is provided in supplementary document (Section II).

4.Conclusion

We investigated the effect of pH, reactant to liquid ratio (R/L) and pyrolysis temperature (PT) on the capacitance of carbon xerogel for applications in capacitive deionization. We showed experimentally that lower density (hence higher porosity) of the electrode does not necessarily increase the capacitance of carbon xerogel. This is potentially due to high volume of macro and micro-size pores in the sample, while higher capacitance (hence the surface area) mostly depends on nano-size pores. Through extensive experimentations and optimization via response surface methodology, we showed that for R/L = 30%, pH = 6.25 and PT = 736, an optimum electrode with capacitance of 42.26 F/g in scan rate of 10 mV/s can be obtained. We synthesized this electrode in the lab, and used it in a batch-mode FCDI cell. We were able to desalinate a brackish water of 1 g/L salt to 87.7% in 6.5 h with SAC of about 7 $mg/g_{electrode}$ which is about 9% higher than commercially available activated carbon material. We further showed that an identical FCDI apparatus can be used for desalination of higher salinity solutions, although - as expected - it takes longer time to achieve the same salt reduction percentage.

References

[1] M.M. Mekonnen, A.Y. Hoekstra, Four billion people facing severe water scarcity, Sci. Adv., 2 (2016) e1500323.

[2] F.a. AlMarzooqi, A.a. Al Ghaferi, I. Saadat, N. Hilal, Application of capacitive deionisation in water desalination: A review, Desalination, 342 (2014) 3–15.
[3] N. Voutchkov, Energy use for membrane seawater desalination – current status and trends, Desalination, 431 (2018) 2–14.
[4] S. Porada, R. Zhao, A. van der Wal, V. Presser, P.M. Biesheuvel, Review on the science and technology of water desalination by capacitive deionization, Prog. Mater. Sci., 58 (2013) 1388–1442.
[5] J.C. Farmer, D.V. Fix, G.V. Mack, R.W. Pekala, J.F. Poco, Capacitive deionization with carbon aerogel electrodes: carbonate, sulfate, and phosphate, in: 27th Int. Soc. Adv. Mater., 1995: pp. 294–304.
[6] T. Yamamoto, T. Nishimura, T. Suzuki, H. Tamon, Control of mesoporosity of carbon gels prepared by sol - gel polycondensation and freeze drying, J. Non. Cryst. Solids, 288 (2001) 46–55.
[7] J. Feng, J. Feng, C. Zhang, Shrinkage and pore structure in preparation of carbon aerogels, J. Sol-Gel Sci. Technol., 59 (2011) 371–380.
[8] Y. Feng, L. Ge, B. Jiang, L. Miao, T. Masaki, Reactant concentration and carbonization to the controllable fabrication of carbon aerogels, Mater. Sci. Forum, 744 (2013) 20–23.
[9] S. Mulik, C. Sotiriou-leventis, N. Leventis, Time-efficient acid-catalyzed synthesis of resorcinol - formaldehyde aerogels, Chem. Mater., 19 (2007) 6138–6144.
[10] J. Li, X. Wang, J. Li, Q. Huang, X. Wang, S. Gamboa, Q. Huang, S. Gamboa, P.J. Sebastian, P.J. Sebastian, Studies on preparation and performances of carbon aerogel electrodes for the application of supercapacitor, J. Power Sources, 158 (2006) 784.
[11] C. Macías, P. Lavela, G. Rasines, M.C. Zafra, J.L. Tirado, C.O. Ania, On the correlation between the porous structure and the electrochemical response of powdered and monolithic carbon aerogels as electrodes for capacitive deionization, J. Solid State Chem., 242 (2016) 21–28.
[12] J. Landon, X. Gao, B. Kulengowski, J.K. Neathery, K. Liu, Impact of pore size characteristics on the electrosorption capacity of carbon xerogel electrodes for capacitive deionization, J. Electrochem. Soc., 159 (2012) A1861–A1866.
[13] D.K. Kohli, S. Bhartiya, A. Singh, R. Singh, M.K. Singh, P.K. Gupta, Capacitive deionization of ground water using carbon aerogel based electrodes, Desal. Water Treat., 57(55) (2016) 26871–26879.
[14] A.M. Elkhatat, S. Al-Muhtaseb, Advances in tailoring resorcinol-formaldehyde organic and carbon gels, Adv. Mater., 23 (2011) 2887–2903.
[15] S.W. Hwang, S.H. Hyun, Capacitance control of carbon aerogel electrodes, J. Non. Cryst. Solids, 347 (2004) 238–245.
[16] A. Halama, B. Szubzda, G. Pasciak, Carbon aerogels as electrode material for electrical double layer supercapacitors - Synthesis and properties, Electrochim. Acta., 55 (2010) 7501–7505.
[17] D. Wu, R. Fu, S. Zhang, M.S. Dresselhaus, Preparation of low-density carbon aerogels by ambient pressure drying, Carbon N. Y., 42 (2004) 2033–2039.
[18] R. Kumar, S.S. Gupta, S. Katiyar, V.K. Raman, K.S. Varigala, T. Pradeep, A. Sharma, Carbon aerogels through organo-inorganic co-assembly and their application in water desalination by capacitive deionization, Carbon N. Y., 99 (2016) 375–383.
[19] D. Wu, R. Fu, Requirements of organic gels for a successful ambient pressure drying preparation of carbon aerogels, J. Porous Mater., 15 (2008) 29–34.
[20] R. Saliger, V. Bock, R. Petricevic, T. Tillotson, S. Geis, J. Fricke, Carbon aerogels from dilute catalysis of resorcinol with formaldehyde, J. Non. Cryst. Solids, 221 (1997) 144–150.
[21] A. Alkhudhiri, N. Darwish, N. Hilal, Membrane distillation: A comprehensive review, Desalination, 287 (2012) 2–18.
[22] H. Pröbstle, M. Wiener, J. Fricke, Carbon aerogels for electrochemical double layer capacitors, J. Porous Mater., 10 (2003) 213–222.
[23] B. Fang, L. Binder, A modified activated carbon aerogel for high-energy storage in electric double layer capacitors, J. Power Sources, 163 (2006) 616–622.
[24] C.J. Gabelich, T.D. Tran, I.H.M. "Mel" Suffet, Electrosorption of inorganic salts from aqueous solution using carbon aerogels, Environ. Sci. Technol., 36 (2002) 3010–3019.
[25] B. Jia, W. Zhang, Preparation and application of electrodes in capacitive deionization (CDI): a state-of-art review, Nanoscale Res. Lett., 11 (2016) 64.
[26] S. Chandrasekaran, P.G. Campbell, T.F. Baumann, M.A. Worsley, Carbon aerogel evolution: Allotrope, graphene-inspired, and 3D-printed aerogels, J. Mater. Res., (2017) 1–20.
[27] N. Job, R. Pirard, J. Marien, J. Pirard, Porous carbon xerogels with texture tailored by pH control during sol – gel process, Carbon N. Y., 42 (2004) 619–628.
[28] M.-F. Yan, L. Zhang, R. He, Z.-F. Liu, Synthesis and characterization of carbon aerogels with different catalysts, J. Porous Mater., (2015) 699–703.
[29] S. Mezzavilla, C. Zanella, C. Della, V. Gian, D. Soraru, Carbon xerogels as electrodes for supercapacitors. The influence of the catalyst concentration on the microstructure and on the electrochemical properties, J. Mater. Sci., 47 (2012) 7175–7180.
[30] M.A. Bezerra, R.E. Santelli, E.P. Oliveira, L.S. Villar, L.A. Escaleira, Response surface methodology (RSM) as a tool for optimization in analytical chemistry, Talanta, 76 (2008) 965–977.
[31] C.H. Fang, P.I. Liu, L.C. Chung, H. Shao, C.H. Ho, R.S. Chen, H.T. Fan, T.M. Liang, M.C. Chang, R.Y. Horng, A flexible and hydrophobic polyurethane elastomer used as binder for the activated carbon electrode in capacitive deionization, Desalination, 399 (2016) 34–39.
[32] K. Laxman, M.T.Z. Myint, H. Bourdoucen, J. Dutta, Enhancement in ion adsorption rate and desalination efficiency in a capacitive deionization cell through improved electric field distribution using zinc oxide nanorods coated activated carbon cloth electrodes, ACS Appl. Mater. Interfaces, 6(13) (2014) 10113–10120.
[33] A.T.U. Nugrahenny, J. Kim, S. Kim, D. Peck, S. Yoon, Preparation and application of reduced graphene oxide as the conductive material for capacitive deionization, Carbon Lett., 15 (2014) 38–44.
[34] F. Ahmad, S.J. Khan, Y. Jamal, H. Kamran, A. Ahsan, M. Ahmad, A. Khan, Desalination of brackish water using capacitive deionization (CDI) technology, Desal. Water Treat., 57(17) (2016) 7659–7666.
[35] A. Leonard, S. Blacher, M. Crine, W. Jomaa, Evolution of mechanical properties and final textural properties of resorcinol – formaldehyde xerogels during ambient air drying, J. Non. Cryst. Solids, 354 (2008) 831–838.

Supplementary

I: Further quality assessment of models

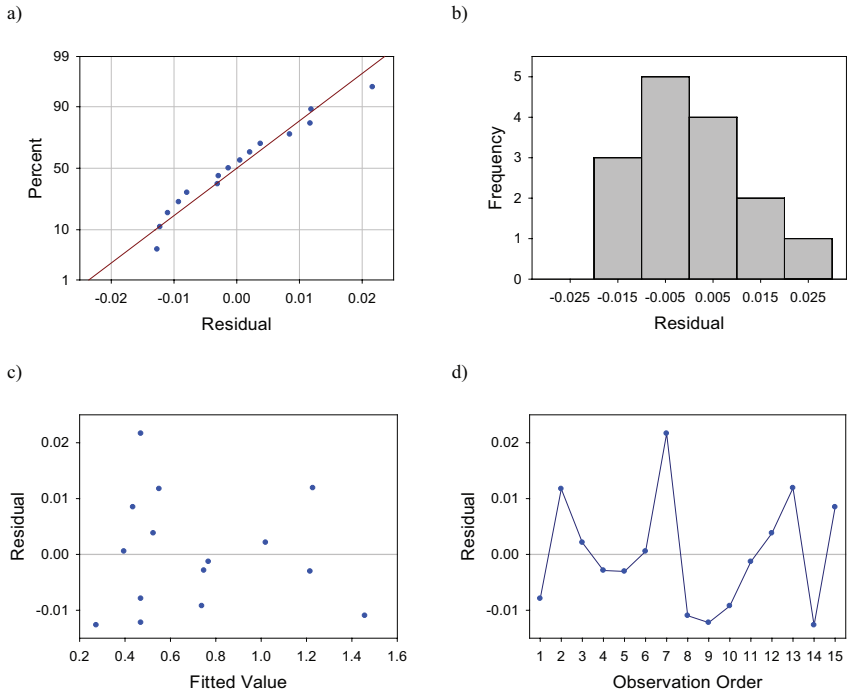

Fig. S1. Residual plots of our introduced model for density a) normal a probability plot, b) histogram of residuals, c) residuals versus fitted values, and d) residuals versus observation orders.

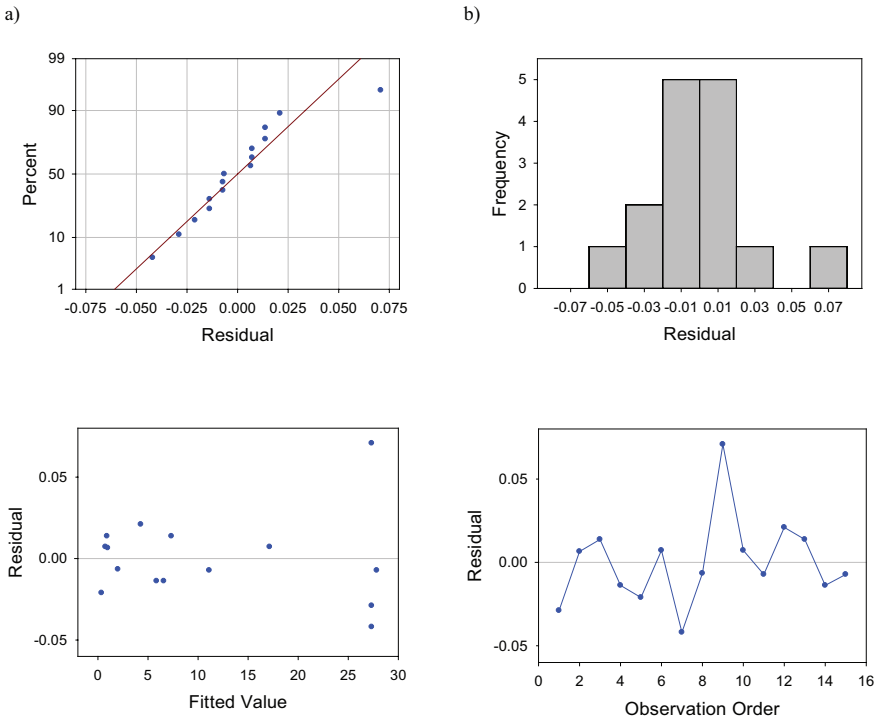

Fig. S2. Residual Plots of our introduced model for capacitance a) normal probability plot, b) histogram of residuals, c) residuals versus fitted values, and d) residuals versus observation orders.

We laid out in Fig. S1(a) the normal probability plot of residuals of our introduced model for density, which shows a very close proximity to a line. This shows that our residuals have a normal distribution. The histogram of residuals further stresses the closeness of the distribution to a normal distribution (Fig. S1(b)). If residuals are plotted against fitted values or observation order (Fig. S1(c,d)), as desired we see a random distribution.

Fig. S2(a) and the histogram shown in Fig. S2(b) show that the residual of our proposed model for capacitance have a normal distribution and Fig. S2(c) and Fig. S2(d) show random distribution of our residuals.

II: Electrical Conductivity measurement during the tests

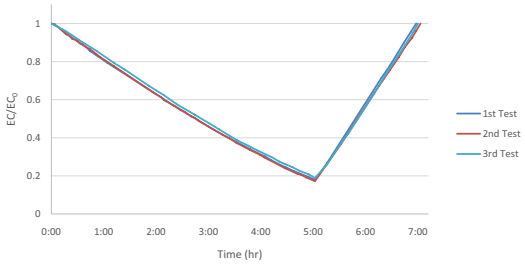

Fig. S3. Variation of electrical conductivity as a function of time for the three tests conducted.